Direct Fabrication of Nanoscale Light Emitting Diode on Silicon Probe Tip for Scanning Microscopy

Kazunori Hoshino, *Member, IEEE*, Lynn J. Rozanski,
David A. Vanden Bout, and Xiaojing Zhang, *Member, IEEE*

***Abstract*—We have fabricated a silicon microprobe integrated with a nanometer-sized light emitting diode (Nano-LED) on the tip. This paper describes the fabrication procedure and preliminary topographic testing results. The silicon probe with electrode pattern was made by wet-etching a Silicon-on-Insulator wafer using oxide as the mask. Subsequently, the probe tip was cut using a Focused Ion Beam (FIB) to form a 150 nm-wide gap. Semiconductor nanoparticles (CdSe/ZnS core-shell nanoparticles) were electrostatically trapped and excited within the electrode gap made on the probe tip. The LED-tip is approximately 150 nm $\times$ 150 nm. The Nano-LED light intensity and current were measured as a function of the driving voltage up to 25 V. In addition to the electroluminescence peaks from the CdSe particles, possible emission from silicon dioxide doped in the FIB milling process was also observed in the measured spectra. Basic mechanical characteristics of the silicon probe were measured by mounting the probe on a tuning fork in a standard near-field scanning optical microscopy (NSOM) set up. It was observed that the drag force reduces the probe oscillation as the vibrating tip approached the near-field of the sample surface. The topographic images of a chromium test pattern on a glass substrate were successfully acquired by keeping the probe tip within roughly 5 nm from the sample surface. Although the probe tip shape and the location of the Nano-LED are yet to be further optimized before realizing near-field optical scanning experiment, the result showed its great promise as a new type of NSOM tip with the "on-probe" light-source. [2007-0111]**

***Index Terms*—Light emitting diodes (LEDs), near-field scanning optical microscopy (NSOM), semiconductor nanoparticles.**

I. Introduction

NEAR-FIELD scanning optical microscopy (NSOM) [1], which combines scanning probe technology with optical microscopy, measures subwavelength optical properties as well as nanoscale topographic properties like a regular atomic force microscope (AFM). The conventional NSOM has a resolution directly related to the size of the probe used, generally a fiber optic pulled to have an aperture with a 50–150 nm diameter. NSOM has been used in almost all optical microscopy applications such as molecular feature characterization of organic films [2], polymers [3] and biomolecules [4], Raman spectroscopy [5], laser ablation patterning [6] and optical recording for data storage devices [7].

Although conventional NSOM is a powerful tool for exploring the nanoscale features of thin films, its large-scale applications in integrated systems are limited due to the manual assembly process of the probe with an illuminating fiber. In addition, an external light source is required for each NSOM probe, further increasing the system complexity. Approaches for miniaturizing NSOM probes include microelectromechanical systems (MEMS) apertures fabricated by the low temperature oxidation and selective etching process [8], and a light absorbing gold particle [9] and a fluorescent bead [10] manually attached on the tips of a drawn glass tube tip and a force sensing cantilever. All of these approaches still require an external laser light source and retain the same problem as mentioned above.

Fabrication of vertical-cavity surface-emitting lasers on the NSOM probes were reported in an attempt to integrate a light source [11], [12], but the light emitting areas were larger than several micrometers and the probes still require a metal coating with an aperture to obtain the diffraction's limited resolution.

Organic Light Emitting Diodes (OLEDs) are promising on-chip light sources since they can be easily integrated on various substrates like flexible thin films [13]. The integration of an OLED on a scanning probe cantilever was reported recently [14], but the size of the resulting LED was approximately 10 μm $\times$ 10 μm, which is too large to work as a near-field light source. Alternatively, semiconductor nanoparticles, such as CdSe/ZnS core-shell quantum dots, are investigated for their electroluminescent properties [15], [16]. Similar to polymer OLEDs, the semiconductor nanoparticle-based light source can be fabricated by spin coating processes. However, unlike the organic-polymer devices, the device lifetime is typically much longer. The CdSe semiconductor nanoparticle LEDs exhibit a size-dependent color variation due to quantum confinement effects [17]. Therefore, the emission wavelength can be tailored simply by choosing the particles of a specific diameter.

Direct fabrication of a nanometer-sized LED has been demonstrated on a patterned Silicon-on-Insulator (SOI) wafer [18]. The fabrication process was a combination of top-down fabrication of a nanometer-sized electrode gap and bottom-up

Manuscript received May 15, 2007; revised September 26, 2007. This work was supported in part by the Wallace H. Coulter Foundation, by the NSF Nanoscale Exploratory Research (NER) Program (ECS-0609413), by the UT Research Grant, the Welch Foundation, and by The Strategic Partnership for Research in Nanotechnology (SPRING). This paper was performed in part at the Microelectronics Research Center at the UT Austin of National Nanofabrication Infrastructure Network supported by National Science Foundation (NNIN-0335765). Subject Editor S. Merlo.

K. Hoshino and X. Zhang are with the Department of Biomedical Engineering, The University of Texas at Austin J. J. Pickle Research Campus, Austin, TX 78758 USA (e-mail: hoshino@mail.utexas.edu; john.zhang@engr.utexas.edu).

L. J. Rozanski and D. A. Vanden Bout are with the Department of Chemistry and Biochemistry and also with the Center for Nano and Molecular Materials Science and Technology, The University of Texas at Austin, Austin, TX 78712 USA (e-mail: rozanski@mail.utexas.edu; davandenbout@mail.utexas.edu).

Color versions of one or more of the figures in this paper are available online at http://ieeexplore.ieee.org.

Digital Object Identifier 10.1109/JMEMS.2007.910254

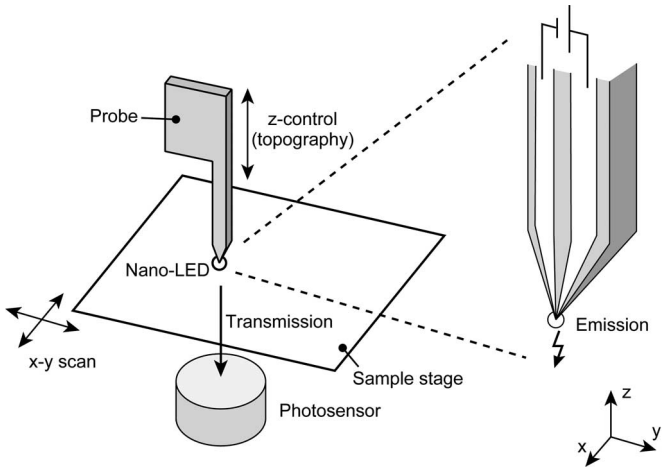

Fig. 1. Diagram of the NSOM setup and proposed silicon probe integrated with Nano-LED.

technique of nanoparticle trapping. The fabrication process is compatible with the silicon-based fabrication techniques used in MEMS. We use this technique to create a nanoscale LED (Nano-LED) on the tip of a MEMS-fabricated probe for near-field optical microscopy applications. In this paper, we describe the detailed fabrication procedures and preliminary topographic testing results for future NSOM application. The proposed silicon probe will be installed in an NSOM setup, as shown in Fig. 1. The probe tip scans the sample surface similar to a regular AFM. The Nano-LED is fabricated on the probe tip. It can be driven by a current supplied from the electrodes and does not require any additional optical components such as lenses, apertures and waveguides. Measured basic characteristics of the fabricated Nano-LED are described in this paper. We also discuss the problems we have to overcome before realizing successful NSOM measurement in the described setup.

II. Design and Fabrication

The silicon probe is made from an SOI wafer with the device, insulation and handle layers having a thickness of 2.2, 1.1 and 185 μm, respectively. The probe body is typically 300 μm wide and 2500 μm long to fit in an NSOM scanning head. Both the device and the handle silicon layers were wet-etched by tetra-methyl-ammonium-hydroxide (TMAH), which resulted in tapered shapes of the probe and electrode tips. Wet-etching procedures are shown in Fig. 2. First, the wafer was wet-oxidized by 300 nm at 1000 °C and patterned with CF_4 Plasma (step 1 in Fig. 2). The device layer was then etched by 25% TMAH at 85 °C for 4 min to form the electrode (step 2 in Fig. 2). The wafer was wet-oxidized again by 300 nm followed by patterning of the back-side etch mask. The wet-etching for the probe body was carried out until the length of the etched probe became approximately 2–3 μm longer than that of the prepatterned electrode (step 4 in Fig. 2). The dimensions of the oxide etch masks are roughly estimated by using an anisotropic crystalline etching simulation (ACES) program [19]. Fig. 3(a) shows the optical micrograph of a fabricated silicon probe with electrode pattern. Fig. 3(b) shows the mask design and

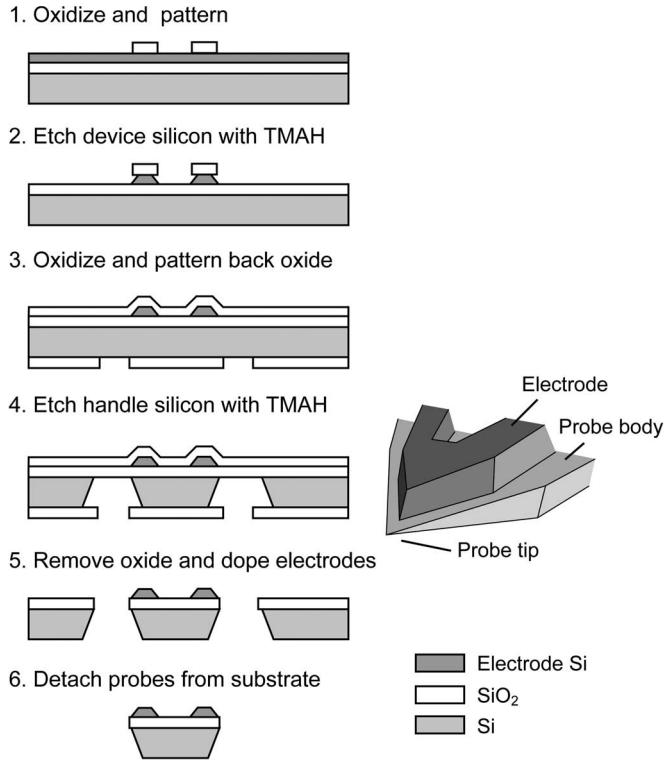

Fig. 2. Fabrication procedure of the MEMS NSOM probe. The probe was made by wet-etching of silicon.

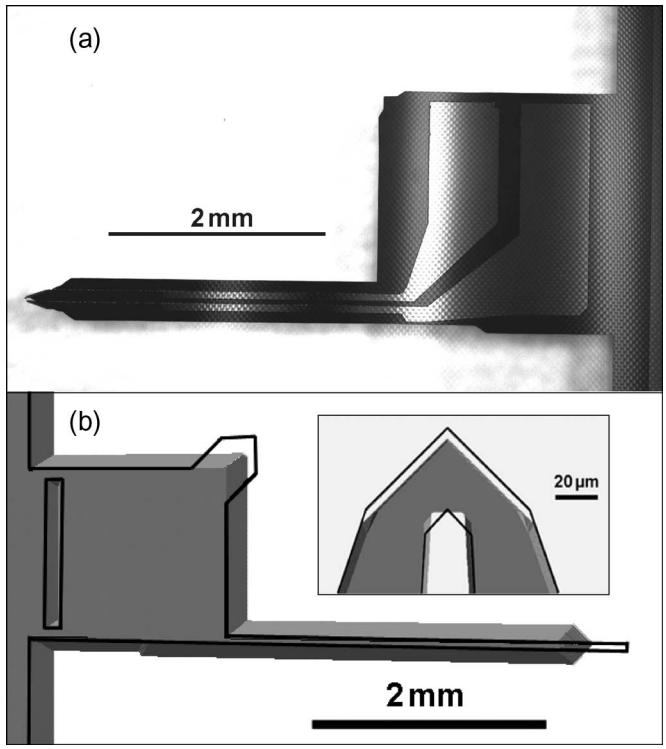

Fig. 3. (a) Photograph of the wet-etched silicon probe. (b) Wet-etching simulation for the electrode and the probe body. The wet etch masks are shown in black lines. Calculation was performed on an ACES program.

the simulation result. The masks are shown in black lines. The electrode was doped by deposition of phosphorous oxychloride for 50 min at 900 °C to obtain higher electrical conductivity

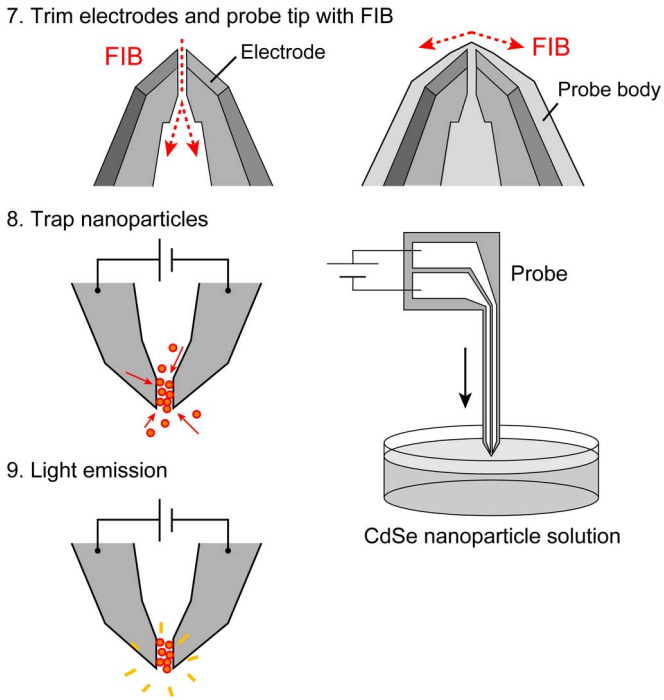

Fig. 4. Fabrication procedure (continued). The electrode and the probe tip were cut with a FIB (step 7). Nanoparticles were then trapped to the electrodes in a toluene solution to make an LED (step 8).

before the probe was detached from the substrate (steps 5 and 6 in Fig. 2).

The fabrication of the nanogap used to attract nanoparticles is shown in Fig. 4. The electrodes and the probe tip were precisely patterned with a focused ion beam (FIB) to form a 150-nm-wide gap about 100–200 nm from the tip of the probe body (step 7 in Fig. 4). Fig. 5 is a Scanning Electron Micrograph (SEM) of the probe and the probe tip with 150-nm-wide gap. The probe is then assembled onto a miniature circuit board through wire-bonding to connect to both the signaling circuitry and power supplies.

The Nano-LED was made by electrostatically trapping semiconductor nanoparticles (CdSe/ZnS core-shell nanoparticles) between the facing electrodes [18] on the probe tip. To trap the nanoparticles, the electrodes were immersed in the toluene solution (step 8 in Fig. 4). When the voltage (typically 5–10 V) was applied, the nanoparticles were polarized and attracted to the gap along the electric field gradient. We prepared particles with the average diameter of 4.8 nm, which has a designed luminescence peak around 550 nm. The probe was then annealed at up to 120 °C for 2 min to dry the organic solvents. Fig. 6(a) shows an SEM photograph of trapped particles in the nanogap. Although the particles cover the entire surface of the electrodes as shown in the figure, the electroluminescence is thought to be emitted from the part where currents go through, i.e., from the bridges made within the gap. Operation of an NSOM probe requires the LED to act as a near-field emitter. The light source should be placed as close as possible to the probe tip. The precise positioning of the nanoparticle bridge relies on the FIB-created nanogap. With the milling precision as shown in Fig. 5 and the multidimensional freedom (x, y, z, rotation and tilt) of the stage in the FIB apparatus (FEI Strata

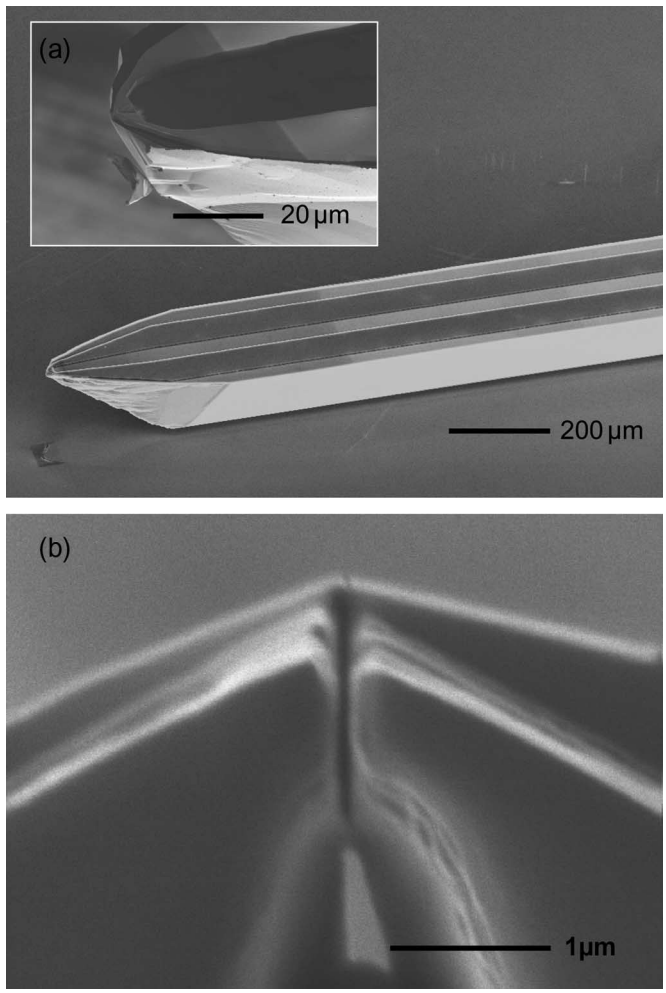

Fig. 5. SEMs of (a) fabricated silicon probes and (b) FIB-cut electrode with a 150 nm-wide gap.

235), positioning a light source within subwavelength distance, i.e., 100–200 nm, is possible. Light emission from the fabricated LED on the probe tip can be clearly observed, as shown in Fig. 6(b).

III. Nano-LED Characterization

The basic parameters of a Nano-LED, made on a flat substrate rather than a probe, were measured. A quartz substrate was used to observe the LED emission from the bottom using an inverted microscope objective. The electrodes were 800-nm-thick CVD polysilicon doped with phosphorous oxychloride and cut with FIB in the same condition as the described Nano-LED on the probe. The dimensions of the electrodes and the other fabrication steps were also kept the same. We can therefore expect the same optical properties such as light intensity–current–voltage characteristic and electro- and photoluminescence spectrum for the probe LED.

Fig. 7 shows current and light intensity as a function of applied voltage measured for the Nano-LED. Both results show clear diode characteristics with the on-voltages at around 15 V. The on-voltages varied from 5 to 100 V in our experiments, largely depending on the gap width and the resistivity of the silicon electrodes. Lower on-voltages were measured for

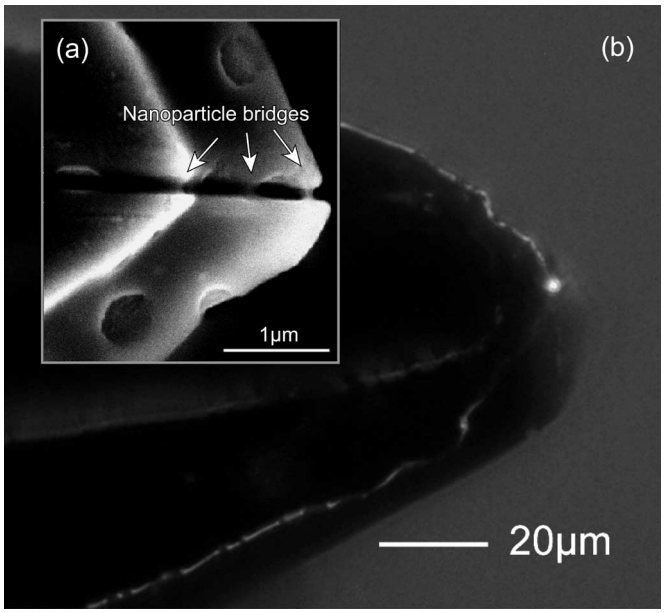

Fig. 6. (a) SEM photograph of trapped particle bridge. (b) Microscopic photograph of the Nano-LED emitting light at a driving voltage of 25 V.

thinner CdSe layers and electrodes with higher conductivities. Driven within a proper voltage range as shown in Fig. 7, the LED showed good repeatability and stability. It was functional after an hour of operation and showed almost the same operating voltages after being kept for a month in atmosphere. No significant intensity change was observed in either case.

Fig. 8(a) shows the electroluminescence spectra of the Nano-LED for different applied voltages. Although the clear linearity of the light intensity–current relationship in Fig. 7 suggests that the emission is electroluminescence, broader emission wavelengths with peaks around 600–700 nm rather than the particle's designed emission of 550 nm were observed. FIB milling of the electrodes and following redeposition of silicon and gallium on the cut area [20] created a highly doped silicon/silicon oxide interface, which is reported to work as a light-emitting diode [21]. In addition to that, the relatively low-lying highest occupied molecular orbital levels of CdSe makes hole injection difficult [22], and as a result, hole-electron recombination rate across the CdSe layer should be lower. Therefore, silicon oxide electroluminescence is one major factor in the broad spectra. Fig. 8(b) shows the electroluminescent spectra of the electrodes before trapping nanoparticles. In Fig. 8(a), one can observe several emission peaks which are not found in Fig. 8(b). These peaks are likely from aggregated CdSe particles which form larger particles. The authors' experiments with larger silicon electrodes, which were patterned with standard RIE, showed several emission cases not only with the wavelength obviously coinciding with the nanoparticle photoluminescence, but also with longer wavelength. An electroluminescence spectrum similar to a photoluminescence peak was also reported for FIB-cut electrodes in [18]. The emission wavelength will be tailored by introducing a silicon fabrication process, such as e-beam lithography, to avoid FIB-induced doping. It is also reasonable to create a layered structure in the LED to improve recombination efficiency. The improvement of the emission efficiency at a specific wavelength in inorganic/organic multilayered nanoparticle LEDs are reported in [15] and [16].

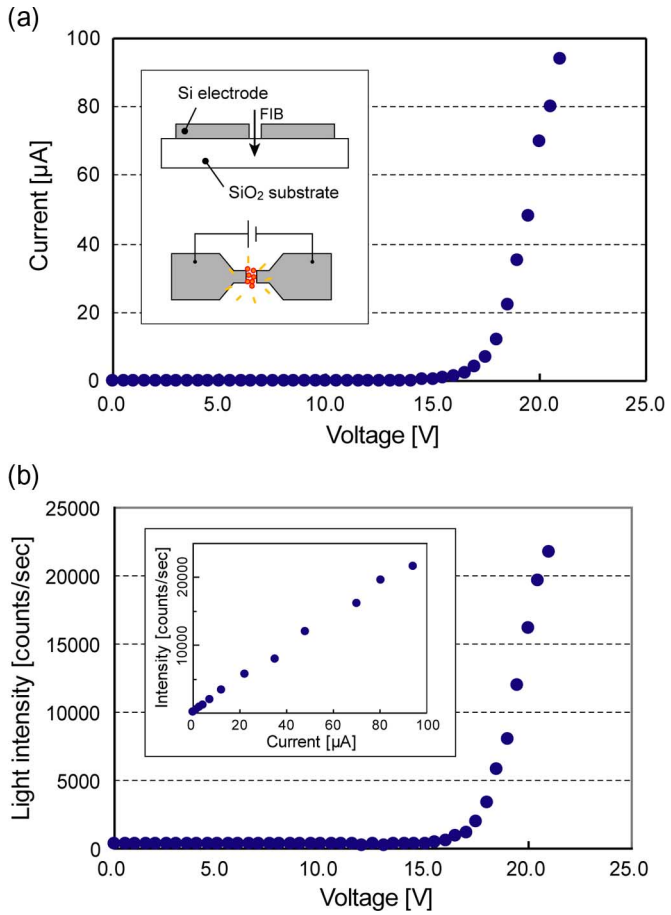

Fig. 7. Optical Characterization of Nano-LED. (a) I–V curve: Current and (b) L–V curve: Light intensity as a function of voltage. L–I curve is also embedded in (b).

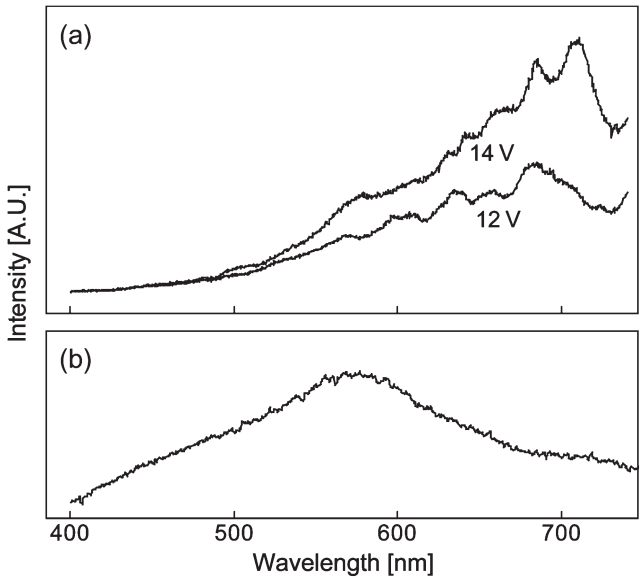

Fig. 8. Electroluminescence spectra of (a) the Nano-LED for different applied voltages and (b) the FIB-cut nanogap without any particles.

In some cases we also see thermal blackbody radiation from silicon electrodes. We found several differences which

discriminate blackbody radiation and the electroluminescence. First, the required current for the blackbody radiation is much larger than the electroluminescence by an order of 10^{2-3}, which results in obvious damage to the silicon electrodes after radiation. The linear relationship between light intensity and current was not observed for the blackbody radiation case. Second, the observed color of the blackbody radiation changes to shorter wavelengths as the applied current increases, which is not the case with the electroluminescence (see Fig. 8 for electroluminescence spectra).

Assuming the emission wavelength is approximately 600 nm to simplify the calculation, emission power p_e of a single photon becomes

$$p_e = h\nu = h \cdot \frac{c}{\lambda} = 3.3 \cdot 10^{-19}\ [\mathrm{J}]. \tag{1}$$

The photon counts of 20 000 [counts/s] at 20 V in Fig. 10(b) defines the emission power as

$$\begin{aligned} p &= p_e \cdot \text{counts} \\ &= (3.3 \times 10^{-19}) \cdot (2.0 \times 10^4) \\ &= 6.6 \times 10^{-15} \quad [\mathrm{W}]. \end{aligned} \tag{2}$$

Since we used a microscope objective with numerical aperture NA $= 0.6(\sin\theta = 0.6)$, the entire emission P of the LED is

$$P = p \cdot (4\pi) \Big/ \left(2\pi \int_0^{\theta/2} \sin\varphi \cdot d\varphi \right) = 2.6 \times 10^{-14}\ [\mathrm{W}]. \tag{3}$$

Thus, the luminous intensity is given by

$$\begin{aligned} \text{Luminous intensity} &= P/4\pi = 2.1 \times 10^{-14}\ [\mathrm{W/sr}] \\ &= 2.0 \times 10^{-11}\ [\mathrm{cd}]. \end{aligned} \tag{4}$$

When we assume the observed LED as a 150 nm $\times$ 150 nm square, the emission area becomes

$$\text{Emission area} = 150\ \mathrm{nm} \times 150\ \mathrm{nm} = 2.3 \times 10^{-14}\ [\mathrm{m}^2]. \tag{5}$$

(5) and (6) give the LED luminance as:

$$\text{Luminance} = 8.7 \times 10^2\ [\mathrm{cd/m}^2]. \tag{6}$$

The result is well within the typical luminance order of $10^1 - 10^3$ reported for OLEDs [23].

IV. Probe Characterization

The probe was tested in an NSOM setup (Veeco Aurora system). The probe was glued to a quartz tuning fork similar to standard fiber tips and mechanically oscillated by a piezoelectric actuator. As the tip approaches the surface of the sample, a drag force acting on the tip changes the probe resonance, measured as a voltage signal from the fork, which in feedback allows the tip to be positioned in the near-field [24]. The typical dimensions of the probe and the fork are shown in Fig. 9. The spring constant of the probe, with dimension of $A = 300\ \mu$m, $B = 50\ \mu$m, $C = 185\ \mu$m, $L = 2500\ \mu$m, is calculated to be

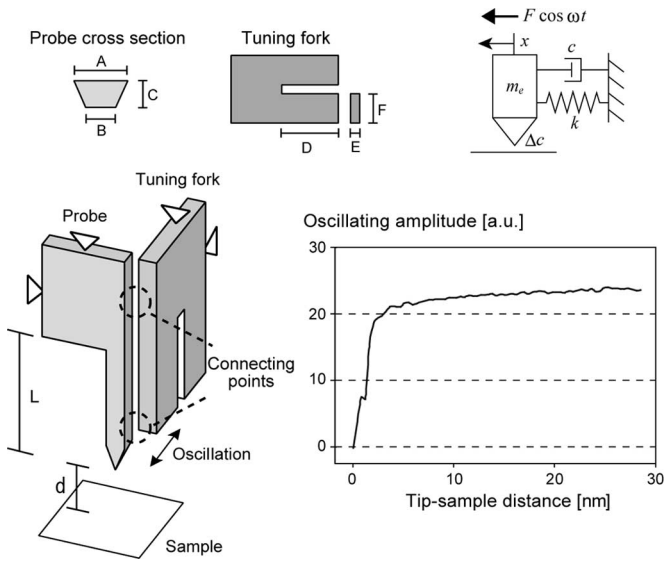

Fig. 9. Force curve measured with a silicon probe. A probe attached to a tuning fork is vibrated by a piezoactuator and the oscillation is monitored as a signal from the fork. A drag force reduces the probe oscillation as the tip approaches within 5 nm to the substrate. Dimensions are typically $A = 300\ \mu$m, $B = 50\ \mu$m, $C = 185\ \mu$m, $D = 1500\ \mu$m, $E = 160\ \mu$m, $F = 400\ \mu$m, $L = 2500\ \mu$m, respectively.

$k_{\mathrm{probe}} = 3800$ [N/m], while that of a prong of the fork, with dimensions of $D = 1500\ \mu$m, $E = 160\ \mu$m, $F = 400\ \mu$m, is calculated to be $k_{\mathrm{fork}} = 120\,000$ [N/m]. With k_{probe} being 3.1% of k_{fork}, the stiffness of the tuning fork is dominant in the probe-attached tuning fork. The resonant frequency of the tuning fork was originally 98.7 kHz and was dampened to 93.0 kHz with the probe attached. The Quality factor Q of the fork attached with the probe was $Q = 147$, which was almost the same as those of forks attached with conventional fiber probes (typically about 150).

We consider the probe-attached tuning fork as a simple mass-spring system experiencing forced oscillation described as:

$$m_e\ddot{x} + c\dot{x} + kx = F\cos\omega t \tag{7}$$

where, m_e, c, k, x, F, and ω are effective mass, viscous coefficient, spring constant, probe displacement, the applied force to the probe, and the angular frequency, respectively (see Fig. 9 for the simplified model). The interaction between the tip and the sample yields an additional drag force $\Delta c\,\dot{x}$ to the equation in the following way:

$$m_e\ddot{x} + (c + \Delta c)\dot{x} + kx = F\cos\omega t. \tag{8}$$

The resonant frequencies of the system (7) and (8) are both given as $\omega_n = \sqrt{k/m_e}$ and the oscillation amplitudes are given as $(F/c\,\omega_n)$ and $F/((c + \Delta c)\omega_n)$, respectively. Since the difference between them only comes from that of the viscous coefficient, change in the oscillating amplitude gives the drag force Δc and thus the tip-sample distance.

A force curve measured with a silicon probe attached to a tuning fork is shown by the graph in Fig. 9. The oscillating amplitudes of the tuning fork were measured as the tip-sample distance d decreased. A sudden decline in oscillation occurred as the tip approaches the surface, and the probe finally ceased

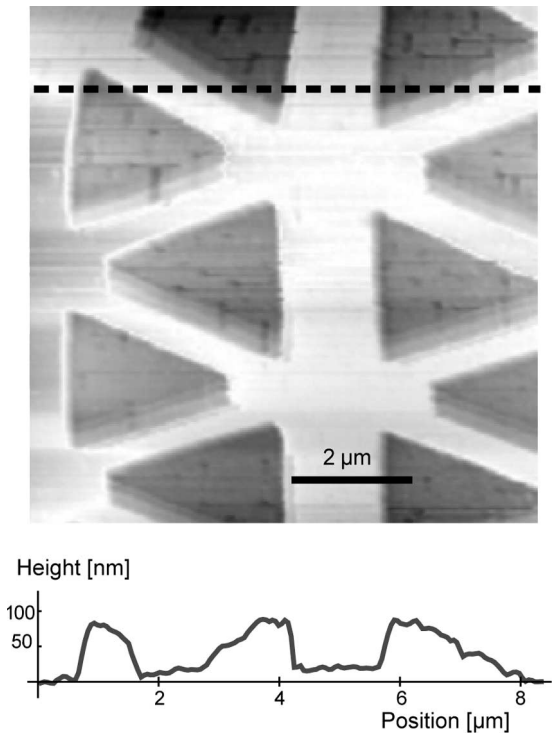

Fig. 10. Topographic image of a test pattern measured with the silicon probe. Section on the dotted line is shown on the bottom.

to oscillate at a certain point. We define the point which gives an amplitude of 0 to be the surface of the sample.

To obtain high-resolution NSOM images, the probe tip must be positioned in the near-field. Topographic images, which are acquired as the probe tip scans the sample, also give important information to complement the optical images. The topographic feature of a chromium test pattern on a glass substrate was measured with a Nano-LED probe as in Fig. 10. During the scan, oscillation amplitude of the tuning fork and the proportional-integral-derivative (PID) parameters were kept almost the same as the case with a standard fiber tip, which indicates that the tip oscillation is in subnanometer order as measured by Normarski differential interferometry and reported in [24]. The probe PID controller was set to maintain the tip-sample distance about 5 nm. A single line scan taken on the dotted line is also shown in Fig. 10. Although the probe successfully traced the patterned triangle structures, an optical signal sufficient for imaging has not been taken. The probe has a rather large tip radius of curvature compared to the dimension of the Nano-LED. It is challenging to create a light source close to an acting probe tip in a well-controlled manner in all three dimensions. For successful near-field imaging applications, a sharper probe tip with a higher aspect ratio should be realized to obtain precise control of the Nano-LED position. Combination of techniques, such as FIB and the doped etch stop technique [25], are currently under investigation to obtain better LED alignment to a tip with a sharper radius of curvature.

V. Conclusion

We have made a nanometer-sized light emitting diode (Nano-LED) through electrostatic assembly of CdSe/Zns core-shell nanoparticles on the tip of a silicon NSOM probe. The basic characteristics of the fabricated Nano-LED were both calculated and measured. The SEM image showed the size of the LED to be 150 nm $\times$ 150 nm. This is as small as the apertures used in commercially available optical fiber probes. The probe was then tested in a standard NSOM setup. The force curve was measured for the fabricated probe, and the probe tip was successfully positioned roughly 5–10 nm from the surface. Although the probe tip fabrication should be further tailored to create a smaller radius of curvature and a more precise location of the Nano-LED to perform successful near-field optical scanning, the probe otherwise fitted well with the system and shows promise as a new type of scanning light tip. The Nano-LED probe holds great promise toward totally integrated "light-source free" optical scanning arrays suitable for novel applications in nanomaterial characterization and biology.

References

[1] B. Hecht, B. Sick, U. P. Wild, V. Deckert, R. Zenobi, O. J. F. Martin, and D. W. Pohl, "Scanning near-field optical microscopy with aperture probes: Fundamentals and applications," *J. Chem. Phys.*, vol. 112, no. 18, pp. 7761–7774, May 2000.

[2] P. F. Barbara, D. M. Adams, and D. B. O'Connor, "Characterization of organic thin film materials with near-field scanning optical microscopy (NSOM)," *Annu. Rev. Mater. Sci.*, vol. 29, pp. 433–469, 1999.

[3] J. Teetsov and D. A. Vanden Bout, "Near-field scanning optical microscopy (NSOM) studies of nanoscale polymer ordering in pristine films of poly(9, 9-dialkylfluorene)," *J. Phys. Chem. B*, vol. 104, pp. 9378–9387, 2000.

[4] M. F. Garcia-Parajoy, J.-A. Veerman, S. J. T. van Noort, B. G. de Grooth, J. Greve, and N. F. van Hulst, "Near-field optical microscopy for DNA studies at the single molecular level," *Bioimaging*, vol. 6, no. 1, pp. 43–53, Mar. 1998.

[5] S. R. Emory and S. Nie, "Near-field surface-enhanced Raman spectroscopy on single silver nanoparticles," *Anal. Chem.*, vol. 69, no. 14, pp. 2631–2635, 1997.

[6] G. Wysocki, S. T. Dai, T. Brandstetter, J. Heitz, and D. Bäuerlec, "Etching of crystalline Si in Cl_2 atmosphere by means of an optical fiber tip," *Appl. Phys. Lett.*, vol. 79, no. 2, pp. 159–161, Jul. 2001.

[7] M. Sasaki, K. Tanaka, and K. Hane, "Cantilever probe integrated with light-emitting diode, waveguide, aperture, and photodiode for scanning near-field optical microscope," *Jpn. J. Appl. Phys.*, vol. 39, no. 12B, pp. 7150–7153, 2000.

[8] P. N. Minh, T. Ono, and M. Esashi, "Nonuniform silicon oxidation and application for the fabrication of aperture for near-field scanning optical microscopy," *Appl. Phys. Lett.*, vol. 75, no. 26, pp. 4076–4078, Dec. 1999.

[9] T. Kalkbrenner, M. Ramstein, J. Mlynek, and V. Sandoghdar, "A single gold particle as a probe for apertureless scanning near-field optical microscopy," *J. Microsc.*, vol. 202, no. 1, pp. 72–76, Apr. 2001.

[10] T. Kan, K. Hoshino, K. Matsumoto, and I. Shimoyama, "Measurement of light intensity field with a fluorescent bead cantilever," in *Proc. IEEE MEMS*, 2006, pp. 822–825.

[11] S. Heisig, O. Rudow, and E. Oesterschulzea, "Scanning near-field optical microscopy in the near-infrared region using light emitting cantilever probes," *Appl. Phys. Lett.*, vol. 77, no. 8, pp. 1071–1073, Aug. 2000.

[12] S. Khalfallah, C. Gorecki, J. Podlecki, M. Nishioka, H. Kawakatsu, and Y. Arakawa, "Wet-etching fabrication of multilayer GaAlAs/GaAs microtips for scanning near-field optical microscopy," *Appl. Phys. A, Solids Surf.*, vol. 71, no. 2, pp. 223–225, 2000.

[13] S. R. Forrest, "The path to ubiquitous and low-cost organic electronic appliances on plastic," *Nature*, vol. 428, no. 6986, pp. 911–918, Apr. 2004.

[14] K. H. An, B. O'Connor, K. P. Pipe, Y. Zhao, and M. Shtein, "Organic light emitting device on a scanning probe cantilever," *Appl. Phys. Lett.*, vol. 89, no. 11, pp. 111 117–111 119, Sep. 2006.

[15] S. Coe, W.-K. Woo, M. Bawendi, and V. Bulovic, "Electroluminescence from single monolayers of nanocrystals in molecular organic devices," *Nature*, vol. 420, no. 6917, pp. 800–803, Dec. 2002.

[16] J. Zhao, J. Zhang, C. Jiang, J. Bohnenberger, T. Basché, and A. Mews, "Electroluminescence from isolated CdSe/ZnS quantum dots

in multilayered light-emitting diodes," *J. Appl. Phys.*, vol. 96, no. 6, pp. 3206–3210, Sep. 2004.
[17] A. P. Alivisatos, "Perspectives on the physical chemistry of semiconductor nanocrystals," *J. Phys. Chem.*, vol. 100, no. 31, pp. 13 226–13 239, 1996.
[18] K. Hoshino, K. Yamada, K. Matsumoto, and I. Shimoyama, "Creating a nano-sized light source by electrostatic trapping of nanoparticles in a nanogap," *J. Micromech. Microeng.*, vol. 16, no. 7, pp. 1285–1289, Jul. 2006.
[19] Z. Zhu and C. Liu, "Micromachining process simulation using a continuous cellular automata method," *J. Microelectromech. Syst.*, vol. 9, no. 2, pp. 252–261, Jun. 2000.
[20] W. Boxleitner and G. Hobler, "FIBSIM—Dynamic Monte Carlo simulation of compositional and topography changes caused by focused ion beam milling," *Nucl. Instrum. Methods Phys. Res. B, Beam Interact. Mater. At.*, vol. 180, no. 1, pp. 125–129, Jun. 2001.
[21] L. Heikkilä, T. Kuusela, and H. P. Hedman, "Electroluminescence in Si/SiO_2 layer structures," *J. Appl. Phys.*, vol. 89, no. 4, pp. 2179–2785, Feb. 2001.
[22] R. A. M. Hikmeta, D. V. Talapin, and H. Weller, "Study of conduction mechanism and electroluminescence in CdSe/ZnS quantum dot composites," *J. Appl. Phys.*, vol. 93, no. 6, pp. 3509–3514, Mar. 2003.
[23] C. Schmitz, M. Thelakkat, and H. W. Schmidt, "A combinatorial study of the dependence of organic LED characteristics on layer thickness," *Adv. Mater.*, vol. 11, no. 10, pp. 821–826, Jul. 1999.
[24] K. Karraia and R. D. Grober, "Piezoelectric tip-sample distance control for near-field optical microscopes," *Appl. Phys. Lett.*, vol. 66, no. 14, pp. 1842–1844, Apr. 1995.
[25] K. Najafi, K. D. Wise, and T. Mochizuki, "A high-yield IC-compatible multichannel recording array," *IEEE Trans. Electron Devices*, vol. ED-32, no. 7, pp. 1206–1211, Jul. 1985.

Kazunori Hoshino (S'99–A'01–M'04) received the B.E., M.E., and Ph.D. degrees in mechanical engineering from the University of Tokyo, Tokyo, Japan, in 1995, 1997, and 2000, respectively.

From 2002 to 2003, he was a Postdoctoral Researcher with the University of Tokyo, where from 2003 to 2006, he was a Lecturer with the Department of Mechano-Informatics. In 2006, he joined The University of Texas at Austin, where he is currently a Research Associate with the Department of Biomedical Engineering. His research interests are MEMS and optical MEMS, biologically inspired microvisual systems, and nanoscale light-emitting devices and nanophotonics.

Lynn J. Rozanski received the B.S. degree in chemistry from the University of Arizona, Tucson, in 2002, and the Ph.D. degree in chemistry from The University of Texas at Austin, in 2007, under the supervision of Dr. D. A. Vanden Bout. Her Ph.D. research focused on the thin-film morphology of conjugated polymer thin films used in LEDs.

She is currently a Postdoctoral Research Scientist with the Commonwealth Scientific and Industrial Research Organisation (CSIRO) Energy Technology, Clayton South, Australia, working with bulk heterojunction solar cells.

David A. Vanden Bout received the B.S. degree in chemistry from Duke University, Durham, NC, in 1990 and the Ph.D. degree in chemical physics from The University of Texas at Austin, in 1995.

He is currently an Associate Professor with the Department of Chemistry and Biochemistry and the Center for Nano and Molecular Materials Science and Technology, The University of Texas at Austin. His research interests include high-spatial-resolution optical microscopy techniques such as near-field scanning optical microscopy and single-molecule spectroscopy.

Xiaojing (John) Zhang (M'04) received the Ph.D. degree in electrical engineering from Stanford University, Stanford, CA, in 2004.

He was with Hewlett-Packard, where he worked on the design of parallel optical interconnects, and with Cisco Systems, where he worked on the design and evaluation of microphotonic devices and optoelectronic subsystems. From 2004 to 2005, he was a Research Scientist with Massachusetts Institute of Technology, Cambridge, and later, he was a visiting Research Associate with the University of Chicago, Chicago, IL. In 2005, he joined the faculty of The University of Texas at Austin, where he is currently an Assistant Professor with the Department of Biomedical Engineering and the Microelectronics Research Center. His research interests include the integration of photonics with microelectromechanical systems and microfluidic devices for *in vivo* imaging, near-field microscopy, and sensing, in particular, toward investigating cellular processes that are critical to development and disease. He is also actively working on nanomicrofabricated photonic sensors for characterizing the cell mechanics, microscanners for molecular imaging and microscopy toward miniaturized endoscopic precancer detection and diagnosis, near-field nanopatterning of biomaterials, hybrid microfluidic-on-silicon instruments for *in vivo* cell and embryo manipulation, culturing and analysis (in particular, microinjections, ultrasonic cellular-scale surgical tools, self-assembly and high-speed particle sorting for studying cellular interactions and embryo development network), and multiscale simulation of fundamental force, flow, energy processes involved in cell-substrate interactions.

Dr. Zhang received the Wallace H. Coulter Foundation Early Career Award for Translational Research in Biomedical Engineering in 2006.